Dmitri Samovski,[1,2] Jingyu Sun,[2] Terri Pietka,[1] Richard W. Gross,[1,3] Robert H. Eckel,[4] Xiong Su,[5] Philip D. Stahl,[2] and Nada A. Abumrad[1,2]

Regulation of AMPK Activation by CD36 Links Fatty Acid Uptake to β-Oxidation

Diabetes 2015;64:353–359 | DOI: 10.2337/db14-0582

Increases in muscle energy needs activate AMPK and induce sarcolemmal recruitment of the fatty acid (FA) translocase CD36. The resulting rises in FA uptake and FA oxidation are tightly correlated, suggesting coordinated regulation. We explored the possibility that membrane CD36 signaling might influence AMPK activation. We show, using several cell types, including myocytes, that CD36 expression suppresses AMPK, keeping it quiescent, while it mediates AMPK activation by FA. These dual effects reflect the presence of CD36 in a protein complex with the AMPK kinase LKB1 (liver kinase B1) and the src kinase Fyn. This complex promotes Fyn phosphorylation of LKB1 and its nuclear sequestration, hindering LKB1 activation of AMPK. FA interaction with CD36 dissociates Fyn from the protein complex, allowing LKB1 to remain cytosolic and activate AMPK. Consistent with this, CD36$^{-/-}$ mice have constitutively active muscle and heart AMPK and enhanced FA oxidation of endogenous triglyceride stores. The molecular mechanism described, whereby CD36 suppresses AMPK, with FA binding to CD36 releasing this suppression, couples AMPK activation to FA availability and would be important for the maintenance of cellular FA homeostasis. Its dysfunction might contribute to the reported association of CD36 variants with metabolic complications of obesity in humans.

AMPK plays an important role in muscle fuel preference and flexibility (1,2). AMPK is normally quiescent, and its activation in response to energy stresses suppresses ATP consumption while upregulating nutrient uptake and catabolism. AMPK activation in muscle involves phosphorylation of the catalytic α-subunit threonine 172 (T172) by upstream kinases, primarily LKB1 (liver kinase B1). Activated AMPK induces sarcolemmal recruitment of the glucose and fatty acid (FA) transporters GLUT4 and CD36 (3), and also upregulates long-chain FA β-oxidation by inactivating acetyl-CoA carboxylase 2, reducing levels of the β-oxidation inhibitor malonyl-CoA. Dysregulation of AMPK signaling in skeletal muscle associates with a diminished capacity to adjust FA oxidation to FA availability, leading to lipid accumulation and insulin resistance (4).

Similar to AMPK, CD36, which facilitates sarcolemmal FA transport, is critical to the adaptive response of muscle FA metabolism. Fasting, muscle contraction, and metabolic signals (FoxO1, AMPK), which are associated with increased energy needs, recruit CD36 to the sarcolemma (3,5). The resulting coordinated increases of FA uptake and oxidation contribute to the adaptability of FA metabolism (3,5,6). The muscle of insulin-resistant humans and that of obese rodents display persistent sarcolemmal CD36 relocation and intracellular lipid accumulation (1).

CD36 plays an important role in modulating events related to lipid use (5). FA binding to CD36 increases levels of cAMP and cytosolic calcium, and mediates taste cell neurotransmitter release for fat taste perception (7) or gut peptide secretions that optimize fat absorption (8).

[1]Department of Medicine, Center for Human Nutrition, Washington University School of Medicine in St. Louis, St. Louis, MO
[2]Department of Cell Biology & Physiology, Washington University School of Medicine in St. Louis, St. Louis, MO
[3]Department of Developmental Biology, Washington University School of Medicine in St. Louis, St. Louis, MO
[4]Department of Endocrinology, Metabolism and Diabetes, University of Colorado, Denver, CO
[5]Department of Biochemistry and Molecular Biology, Medical College of Soochow University, Suzhou, People's Republic of China

Corresponding author: Dmitri Samovski, dsamovsk@dom.wustl.edu, or Nada A. Abumrad, nabumrad@dom.wustl.edu.

Received 9 April 2014 and accepted 11 August 2014.

D.S. and J.S. contributed equally to this work.

In the current study, we examined the possibility that sarcolemmal CD36 signaling might engage AMPK to coordinate FA uptake and oxidation.

RESEARCH DESIGN AND METHODS

Reagents

FA-free BSA, sodium palmitate, and other chemicals were from Sigma-Aldrich (St. Louis, MO); and human highly oxidized LDL (oxLDL) was from Kalen Biomedical (Montgomery Village, MD). All phospho-antibodies were from Cell Signaling Technology (Danvers, MA), anti-Fyn was from Santa Cruz Biotechnology (Santa Cruz, CA), GAPDH was from Sigma-Aldrich, and anti-LKB1 was from Millipore (Billerica, MA). IRDye800 anti-rabbit or anti-goat IgG and IRDye700 anti-mouse IgG were from Rockland (Gilbertsville, PA). Anti-human and anti-mouse CD36 were from R&D Systems (Minneapolis, MN), rat monoclonal anti-mouse CD36 was from AbD Serotec (Raleigh, NC), and mouse monoclonal anti-human CD36 was from Abcam (Cambridge, MA). Alexa Fluor IgGs (594 anti-rabbit, 488 goat anti-mouse, and 488 donkey anti-goat) were from Life Technologies. Mouse CD36 small interfering RNAs (siRNA) (siCD36–1: 5′-AAACCCAGATGACGTGGC AAA-3′; siCD36–2: 5′-AACGACATGATTAATGGCACA CCTGTCTC–3′) were from Life Technologies; and pcDNA3-FLAG-LKB1 (catalog #8591), pRK5 c-Fyn (catalog #16032), and pRK5 DN-Fyn (catalog #16033) were from Addgene.

Mice

Age-matched (3- to 4-month-old), male, wild-type (WT) C57BL/6 and CD36$^{-/-}$ mice (9) backcrossed onto the C57BL/6 line for more than seven generations were fed ad libitum or fasted for 18 h. All protocols were approved by the Animal Studies Committee of Washington University.

Respiratory quotient (RQ; Vco_2/Vo_2 ratio) was determined by indirect calorimetry (ULTRAMAT/OXYMAT 6 analyzer; Siemens) (10), heart triglyceride (TG) content was determined by multidimensional mass spectrometry (TSQ Quantum Ultra mass spectrometer; Thermo Electron) (11), and quadriceps TG content was determined using a kit from Wako Diagnostics (Richmond, VA).

Cells

C2C12 myoblasts grown in high-glucose DMEM with 10% FBS (Life Technologies) supplemented with L-glutamine (2 mmol/L) were differentiated in DMEM containing 2% horse serum. CD36 knockdown in C2C12 myotubes used transfection (Lipofectamine RNAiMAX) with siRNAs (20 nmol/L final), anti-mouse CD36 (Life Technologies), or anti-GFP (controls). All siRNA-transfected myotubes appeared morphologically normal and were used 72 h after transfection.

CHO cells stably expressing CD36 (12) were transiently transfected (Lipofectamine 2000; Life Technologies) then 48 h later were serum starved and treated as indicated. C2C12 myotubes or CHO cells were serum starved (16–18 h) in buffer A (low-glucose, 5 mmol/L DMEM with 2 mmol/L L-glutamine, 100 μmol/L MEM nonessential amino acids, 100 units/mL penicillin, and 100 μg/mL streptomycin). FAs were added with BSA at a ratio of 2:1.

Western Blots and Coimmunoprecipitations

Tissue extracts and cells were lysed (30 min) in ice-cold buffer containing 60 mmol/L Octyl (octylβ-D-glucopyranoside) or 1% Brij99 (polyoxyethylene [20]-oleylether) when indicated. For immunoprecipitation (IP), equal amounts of lysate proteins were incubated (4°C) with antibodies overnight before adding protein G or A agarose beads (Thermo Scientific) (1–3 h). After five washes with cold lysis buffer, bound proteins were eluted by boiling for 5 min in SDS sample buffer, and cleared (10,000*g*, 3 min) supernatants were resolved by SDS-PAGE.

For immunofluorescence (IF), cells grown on coverslips were fixed with ice-cold methanol (−20°C, 20 min), blocked (1 h, PBS with 0.05% Tween 20, 1% BSA, 5% goat serum) at room temperature, and incubated overnight with primary antibodies then for 1 h with Alexa Fluor 488 and/or 594 secondary antibodies. Images were acquired using an inverted microscope (Axiovert 200 M; Zeiss, Thornwood, NY) and ImageJ software (National Institutes of Health).

Palmitate-Supported Cell Respiration

Palmitate (100 μmol/L, 2:1 with BSA)-supported respiration was measured in intact or digitonin (Dig)-permeabilized (10 μg/10^{-6} cells) C2C12 myotubes (Oxygraph-2k; OROBOROS Instruments) at 37°C with room air saturation (13). Cells were serum starved for 16 h, trypsinized, and resuspended in DMEM buffer A (for intact cells) or in MIR05 buffer with 1 mmol/L ATP, 5 mmol/L ADP, 2 mmol/L malate, and 2 mmol/L L-carnitine (for permeabilized cells) (13).

Statistics

Statistical significance was determined using an unpaired Student *t* test or one-way ANOVA followed by Tukey post hoc test for multiple comparisons.

RESULTS

CD36 Regulates AMPK Activation in Myotubes

Long-chain FA addition (1 h) to L6 myotubes enhanced LKB1-mediated AMPK phosphorylation (14). In C2C12 myotubes, we confirmed that 5- to 15-min incubations with palmitic acid (PA) enhance T172 phosphorylated AMPK (pAMPK) and S79 phosphorylation of the AMPK target acetyl-CoA carboxylase 2 (data not shown). We examined the CD36 dependence of AMPK activation by FA using two siRNAs, siCD36–1 and siCD36–2, which markedly reduced CD36 levels (Fig. 1*A*). CD36 knockdown robustly increased pAMPK, suggesting that CD36 expression suppresses AMPK phosphorylation (Fig. 1*A*).

Palmitate addition increased pAMPK levels in control myotubes, but not in CD36-depleted myotubes where basal pAMPK was already high (Fig. 1*B*). Similar results were obtained with oleate (data not shown). CD36 knockdown decreased PA-supported respiration by myotubes

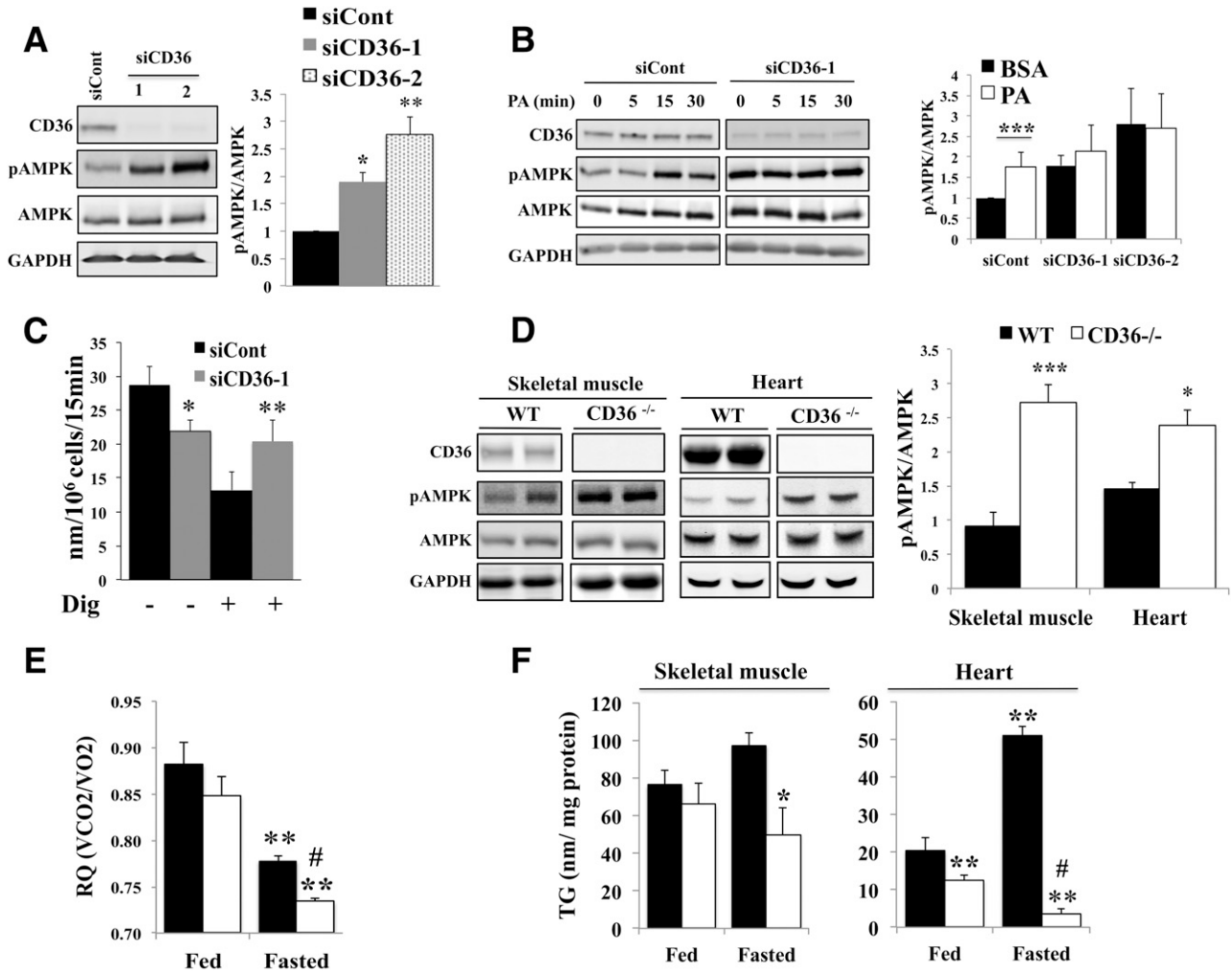

Figure 1—CD36 regulates AMPK phosphorylation and FA oxidation. *A*: CD36 depletion increases AMPK phosphorylation in myotubes. C2C12 myotubes were transfected with CD36-targeted siRNA (siCD36–1 and siCD36–2) or with a nonspecific siRNA (siCont). Knockdown efficiency relative to siCont: 85% ± 0.74, $n = 4$, $P < 0.01$ for siCD36–1; and 66% ± 2.9, $n = 4$, $P < 0.01$ for siCD36–2. Cells were serum starved for 16 h in DMEM buffer A containing 5 mmol/L glucose (see RESEARCH DESIGN AND METHODS). Levels of CD36, pAMPK (T172), AMPK, and GAPDH were measured in cell lysates by immunoblotting. Graph shows the quantification by densitometry of pAMPK (T172)/AMPK as a fold change of siCont. Data are reported as the mean ± SE from four experiments. *$P < 0.05$, **$P < 0.01$, relative to siCont. *B*: CD36 is required for FA-induced AMPK activation. C2C12 myotubes treated with siCont or siCD36 were serum starved for 16 h in DMEM buffer A, incubated with 300 μmol/L PA (2:1 with BSA) or BSA (0 min) for the indicated times, and cell lysates were probed for CD36, pAMPK (T172), AMPK, and GAPDH. Graph shows the quantification of pAMPK (T172)/AMPK in cells treated with PA for 15 min as the fold change of levels in siCont. Data are reported as the mean ± SE from three experiments. ***$P < 0.001$, relative to siCont. *C*: CD36 depletion increases FA oxidation. C2C12 myotubes were starved for 16 h and processed for FA oxidation (see RESEARCH DESIGN AND METHODS). Plots show PA-supported oxygen consumption (nmol/10^6 cells/15 min) for intact or Dig-permeabilized myotubes (siCont or CD36 depleted). Data are reported as the mean ± SE from five experiments. **$P < 0.01$, *$P < 0.05$ relative to the corresponding siCont. *D*: CD36 deletion increases AMPK phosphorylation in vivo. Skeletal muscle (gastrocnemius) and hearts, isolated from WT or CD36$^{-/-}$ mice fasted for 18 h were lysed and probed for CD36, pAMPK (T172), AMPK, and GAPDH for skeletal muscle or β-actin for heart (label omitted for clarity). Graph shows the quantification of pAMPK/AMPK levels in gastrocnemius muscle ($n = 6$ mice) and heart ($n = 4$ mice). Data are reported as the mean ± SE. ***$P < 0.001$, *$P < 0.05$ relative to WT mice. *E*: CD36 deletion increases FA oxidation in vivo. RQs were measured by indirect calorimetry for WT and CD36$^{-/-}$ mice under ad libitum feeding (18 h) and then during 18 h of fasting. Averaged RQs of fed or fasted WT and CD36$^{-/-}$ mice are shown. Data are reported as the mean ± SE. Significance reflects comparisons to fed WT mice (**$P < 0.01$) or fasted WT mice (#$P < 0.01$; $n = 6$ per group). *F*: Endogenous TG stores are depleted in CD36-deficient muscle. Left panel: Quadriceps TG content in WT and CD36$^{-/-}$ mice that had been fed or fasted for 18 h. *$P < 0.05$ compared with fasted WT mice ($n = 6$ per group). Right panel: Myocardial TG content in WT and CD36$^{-/-}$ mice fed or fasted for 18 h. Comparisons are to fed WT mice (**$P < 0.01$) or fasted WT mice (#$P < 0.01$; $n = 5$ per group). All data are reported as the mean ± SE.

(Fig. 1*C*), which is consistent with its impairing FA uptake (3,5). However, knockdown increased respiration when myotubes were permeabilized with Dig (13) to bypass CD36-mediated FA uptake (Fig. 1*C*), which is consistent with knockdown enhancing FA oxidation. Thus, CD36 depletion increases basal pAMPK and FA oxidation. In non-depleted cells, AMPK activation by exogenous FA requires CD36.

Enhanced AMPK Phosphorylation and FA Oxidation From Endogenous TG in Muscle of CD36$^{-/-}$ Mice

AMPK phosphorylation was increased in skeletal muscle (quadriceps) and heart from CD36$^{-/-}$ mice fasted for 18 h compared with WT mice (Fig. 1*D*), indicating that CD36 deletion activates muscle AMPK in vivo. Since CD36 deficiency reduces the availability of exogenous FA for oxidation (3), we examined whether AMPK activation would enhance FA oxidation from endogenous stores. We first compared the RQ (ratio of CO_2 produced to O_2 consumed) of fed and fasted (18 h) WT and CD36$^{-/-}$ mice (Fig. 1*E*). RQ was similar across genotype in the fed state, as previously reported (10), but fasting-induced reduction of RQ was significantly more pronounced in CD36$^{-/-}$ mice (Fig. 1*E*), which is consistent with enhanced FA oxidation.

We next measured muscle TG content. Fed CD36$^{-/-}$ mice had lower myocardial TG content than WT mice, while quadriceps TG content was similar (Fig. 1*F*). Fasting increased the TG content of WT hearts 2.6-fold, as previously reported (15), while TG content of CD36$^{-/-}$ hearts decreased (Fig. 1*F*). Quadriceps TG content trended higher in WT mice, whereas it decreased in CD36$^{-/-}$ mice (Fig. 1*F*). This suggested that in the fasted CD36$^{-/-}$ mouse muscle, endogenous lipids support FA oxidation, depleting intramuscular TG content.

CD36 Regulates LKB1 Subcellular Localization

Several kinases phosphorylate LKB1, the major AMPK kinase in muscle, including the src kinase Fyn (16), which interacts with CD36. Fyn tyrosine phosphorylates LKB1, resulting in its nuclear sequestration and reduced access

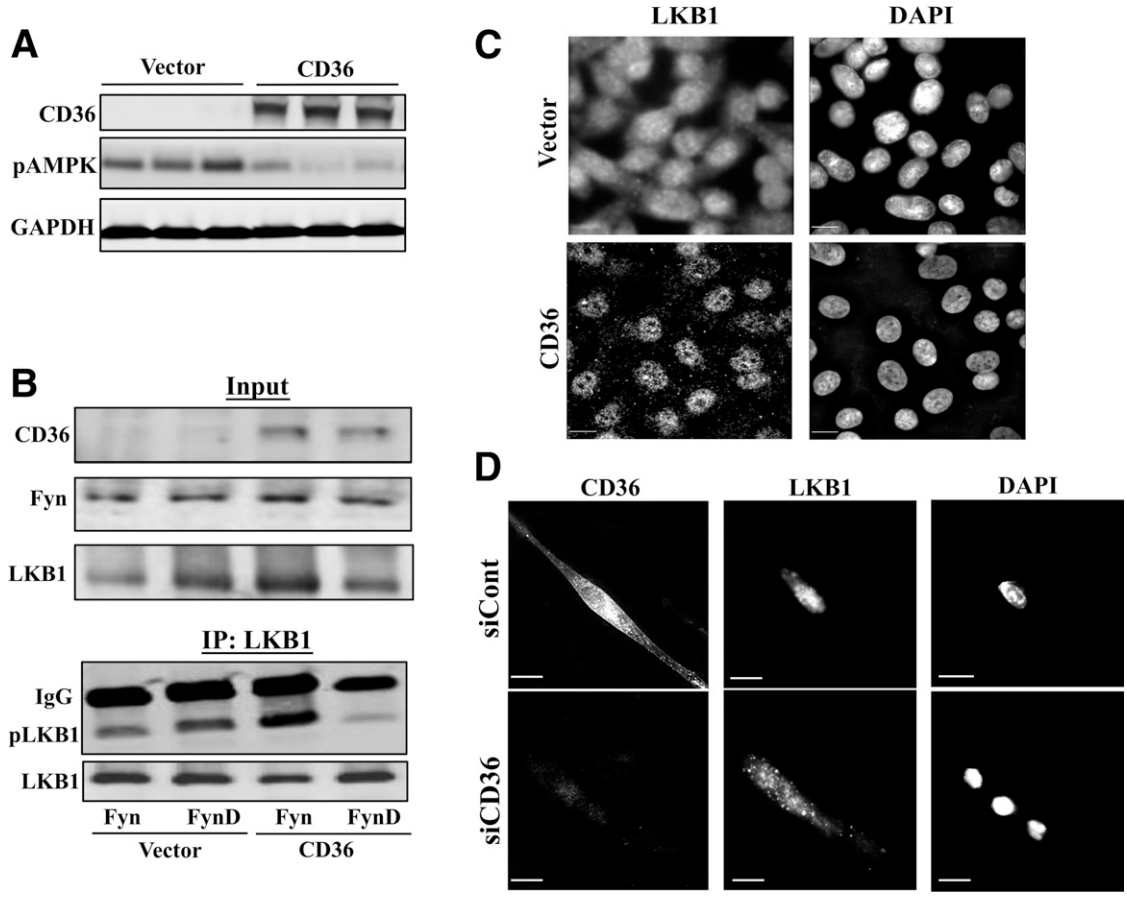

Figure 2—CD36 regulates AMPK activation via Fyn-dependent nuclear sequestration of LKB1. *A*: Suppression of AMPK phosphorylation by CD36 expression. CHO cells lacking CD36 (Vector) or stably expressing CD36 (CHO-CD36) were serum starved (for 16 h in DMEM buffer A), lysed, and probed (in triplicate) for CD36, pAMPK (T172), and GAPDH. Data are representative of two experiments. *B*: Fyn phosphorylation of LKB1 is enhanced by CD36 expression. Control (Vector) and CD36-expressing cells (CD36) were transiently transfected with Fyn or FynD; and serum-starved and cell lysates (Input) were probed for CD36, LKB1, and Fyn. LKB1 was immunoprecipitated from cell lysates using mouse monoclonal antibody for LKB1 (clone 5c10; Millipore). LKB1 immunoprecipitates (IP:LKB1) were probed with phosphotyrosine PY100 (pLKB1) and LKB1 antibodies. *C*: CD36 expression induces nuclear sequestration of LKB1 in CHO cells. CHO cells stably expressing CD36 or Vector controls were serum starved, fixed, and processed for IF as described in RESEARCH DESIGN AND METHODS. The cells were stained with mouse monoclonal LKB1 antibody (clone 5c10; Millipore) and with DAPI to visualize the nuclei. Images are representative of multiple fields from three experiments. Scale bar, 10 μm. *D*: CD36 depletion in C2C12 myotubes abolishes nuclear sequestration of LKB1. C2C12 myotubes treated with siCD36 or siCont were serum starved for 16 h in DMEM buffer A. LKB1 and CD36 were detected using mouse monoclonal anti-LKB1 (5c10; Millipore) and rat monoclonal anti-CD36 antibodies (MF3; AbD Serotec). Images are representative of multiple fields from three experiments. Scale bar, 10 μm.

to cytosolic AMPK (16). We examined the effect of CD36 expression on LKB1 phosphorylation and its Fyn dependence using CHO cells stably expressing CD36 and transiently transfected with native Fyn or dominant-negative Fyn (FynD) (17). CD36 expression reduced pAMPK levels (Fig. 2*A*). LKB1 IP (Fig. 2*B*) and probing with PY100 phosphotyrosine antibody showed increased phosphorylated LKB1 in CD36 cells transfected with Fyn, and this increase was abolished in cells expressing FynD. Thus, CD36 expression promotes Fyn-dependent LKB1 phosphorylation.

IF in CHO (Fig. 2*C*) and HeLa cells (data not shown) with or without stable CD36 expression showed that CD36 promotes nuclear LKB1 localization. LKB1 was distributed throughout the cytoplasm in controls (Fig. 2*C*, top panels) but was predominantly nuclear in CD36 cells (Fig. 2*C*, bottom panels) (nuclear/cytosolic LKB1 in controls and CD36 cells, respectively: 0.25 ± 0.02 and 1.20 ± 0.06; $P < 0.001$). CD36 regulation of LKB1 was observed in C2C12 myotubes (Fig. 2*D*). In controls, LKB1 was mostly nuclear (Fig. 2*D*, top panels), while CD36 depletion redistributed LKB1 to the cytosol (Fig. 2*D*, bottom panels). FA addition (PA, 15 min) to CHO-CD36 cells (Fig. 3*A*) redistributed LKB1 from the nucleus to cytosolic structures that coincided with CD36 (Fig. 3*A*, inset). Similar PA redistribution of LKB1 occurred in HeLa (data not shown) and in C2C12 cells (Fig. 3*B*). Thus, FA addition recruits LKB1 from nuclei to cytosolic CD36-positive vesicles.

CD36 Associates With LKB1, Fyn, and AMPK, and Fyn Is Displaced by Addition of FA, But Not oxLDL

The LKB1-CD36 association was confirmed by CD36 IP in CHO-CD36 cells (Fig. 3*C*) solubilized with Brij99, which preserves hydrophobic interactions between membrane proteins, including CD36 (18). CD36 IP contained LKB1, and content was increased by palmitate. Flotillin-1, a lipid raft marker, was recovered from CD36 IP, suggesting that the CD36-LKB1 association might occur in lipid rafts

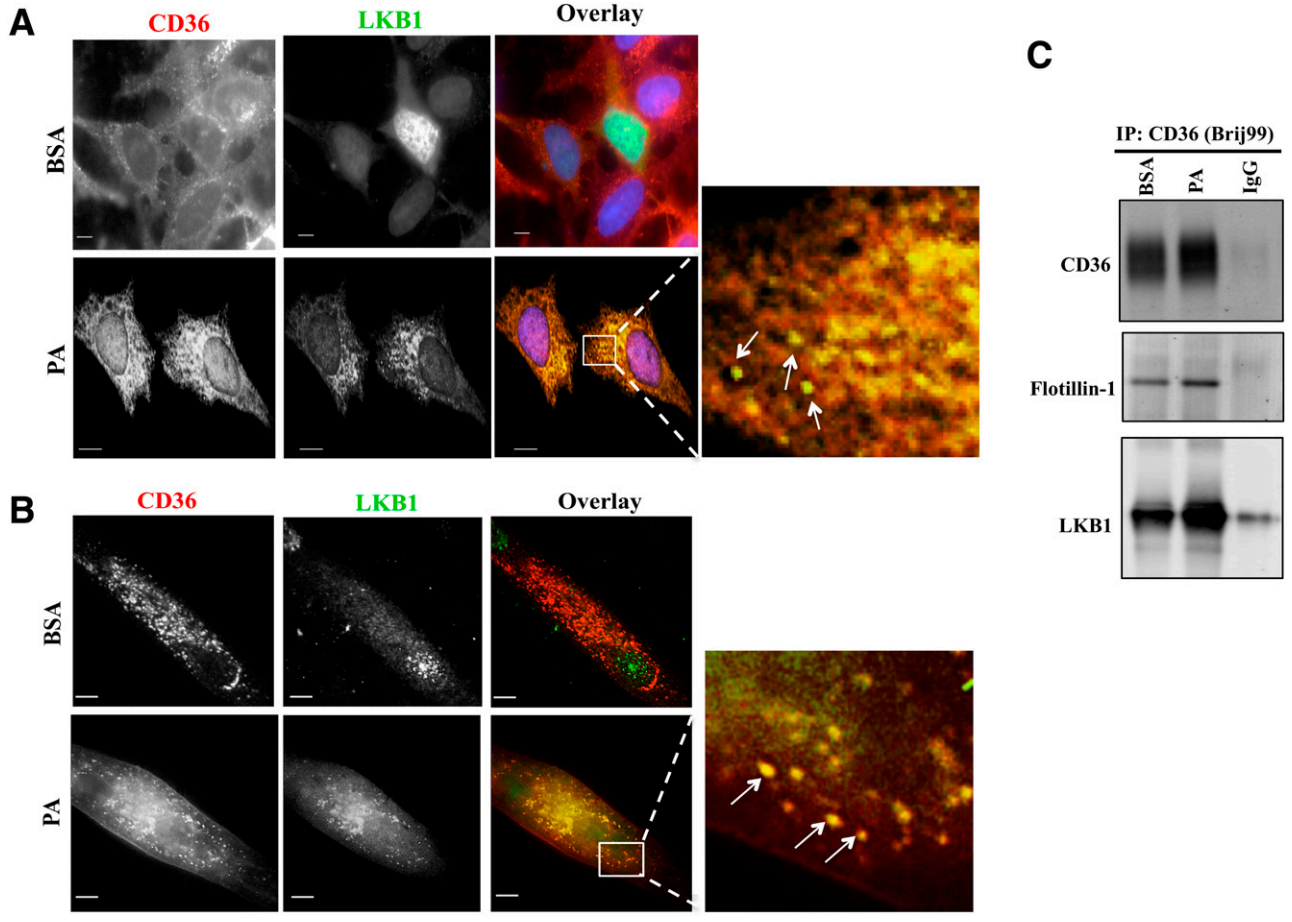

Figure 3—PA induces CD36 association with LKB1. *A* and *B*: PA addition relocates LKB1 to cytosolic CD36-positive vesicular structures. Micrographs showing PA-induced redistribution of LKB1 and its colocalization with CD36 in CHO-CD36 cells (*A*) and in myotubes (*B*). The cells were serum starved, incubated with 300 μmol/L PA (2:1 BSA) or BSA for 15 min, and stained with anti-CD36 (FA6-152 [Abcam] for CHO; MF3 [AbD Serotec] for myotubes) and anti-LKB1 (5c10; Millipore) antibodies. Images are representative of multiple fields from three experiments. Arrows point to overlap between CD36 and LKB1 within cytoplasmic vesicular structures. Scale bar, 10 μm. *C*: PA addition results in a CD36-LKB1 association within lipid domains. CHO-CD36 cells, serum starved then incubated with 300 μmol/L PA (2:1 BSA) or BSA for 15 min were lysed with buffer containing 1% Brij99. Equal protein amounts were immunoprecipitated (IP:CD36) using anti-CD36 antibody (AF1955; R&D Systems) and nonimmune IgG as a negative control. Immunoprecipitates were resolved by SDS-PAGE, and probed for CD36, flotillin-1, and LKB1. Data are representative of two experiments.

(Fig. 3*C*). CHO-CD36 cells were then solubilized with Octyl, which efficiently extracts membrane proteins (19) (Fig. 4). Flotillin-1 was then absent from CD36 IP (Fig. 4*A*), but LKB1 was still recovered, and PA increased this recovery (Fig. 4*B*). These data supported CD36-LKB1 association independent of membrane lipid domains and FA enhancement of this interaction.

We next examined whether the effect of FA on LKB1 might involve modulation of the CD36 association with Fyn, and potentially with AMPK. The CD36 ligand oxLDL enhances CD36 association with src kinases in platelets (20). The effect of FA is unknown, so CD36 immunoprecipitates from CHO-CD36 cells incubated with or without PA or oxLDL were probed for coassociated Fyn and AMPK.

The addition of palmitate did not alter the amounts of Fyn found in cell lysates (Fig. 4*B*), but markedly decreased Fyn recovery in CD36 IP, suggesting a reduced CD36-Fyn association. AMPK was identified in CD36 IP, and its recovery increased after PA (Fig. 4*B*). In contrast to PA, incubation of CD36-expressing cells with oxLDL (Fig. 4*C*) increased the amount of Fyn pulled down by CD36, as in platelets (20), without altering the amount of LKB1 recovered. Thus, PA addition specifically decreases the CD36-Fyn interaction while increasing the CD36-LKB1-AMPK interaction.

DISCUSSION

Our findings support CD36 control of LKB1 and AMPK activity, which might have relevance to the maintenance of cellular FA homeostasis. CD36 regulation of AMPK appears to be linked to optimal AMPK responsiveness to FA supply and is exerted through the assembly of a CD36/Fyn/LKB1/AMPK protein complex (Fig. 4*D*). Under low exogenous FA availability, this complex maintains quiescence of AMPK by

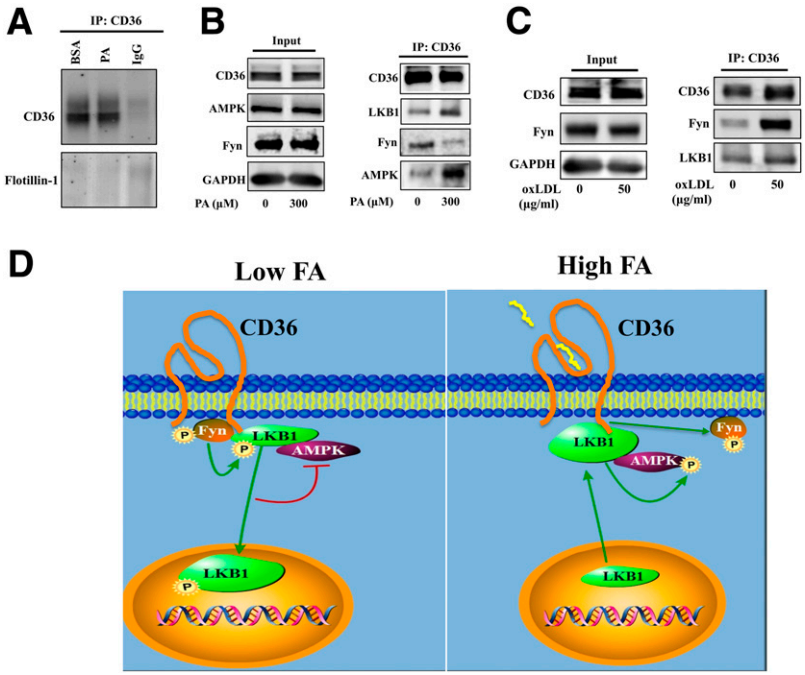

Figure 4—FA and oxLDL differentially regulate the association of CD36 with Fyn, LKB1, and AMPK. *A* and *B*: PA reduces the CD36 association with Fyn, while enhancing the association with LKB1 and AMPK. CHO-CD36 cells transiently transfected with Fyn were serum starved, incubated for 15 min with 300 μmol/L PA (2:1 with BSA) or BSA, and lysed with buffer containing 60 mmol/L Octyl. *A*: Equal amounts of protein were immunoprecipitated using anti-CD36 antibody and nonimmune IgG as a negative control. Immunoprecipitates were resolved by SDS-PAGE, and incubated with antibodies for CD36 and flotillin-1. Data are representative of two experiments. *B*: Immunoblots of cell lysates (input) were resolved by SDS-PAGE, and probed for CD36, pAMPK (T172), AMPK, Fyn, and GAPDH. CD36 immunoprecipitates (IP:CD36) were probed for CD36, Fyn, LKB1, and AMPK. Data are representative of three experiments. *C*: oxLDL enhances CD36 association with Fyn. CHO-CD36 cells transiently transfected with Fyn were serum starved and incubated for 15 min with 50 μg/mL oxLDL, then were lysed with buffer containing Octyl. Cell lysates (Input) were probed for CD36, pAMPK (T172), AMPK, Fyn, and GAPDH. CD36 immunoprecipitates were probed for CD36, Fyn, LKB1, and AMPK. Data are representative of three experiments. *D*: Schematic representation of the mechanism for AMPK regulation by CD36 and FA. A ternary protein complex composed of Fyn, LKB1, and AMPK is assembled with CD36. When exogenous FA concentrations are low (left panel), CD36-bound Fyn can access and phosphorylate (P) LKB1, which induces LKB1 nuclear relocation and reduces the amount of cytosolic LKB1 available to activate AMPK. As a result AMPK is kept quiescent. When exogenous FA concentrations rise (right panel), the enhanced FA interaction with CD36 promotes Fyn dissociation from the protein complex, hindering the access of Fyn to phosphorylate CD36-associated LKB1. The ensuing enrichment in cytosolic LKB1 activates AMPK, which enhances FA oxidation by inactivating acetyl-CoA carboxylase. AMPK also induces cell surface CD36 recruitment (3,5). Thus, the CD36-AMPK pathway integrates FA uptake and FA catabolism. When CD36 is depleted, the lack of nuclear sequestration of LKB1 results in constitutively active AMPK that cannot be further activated by FA. The data suggest that CD36 dysfunction impairs AMPK lipid-sensing ability.

promoting Fyn-dependent LKB1 phosphorylation and LKB1 relocation to the nucleus. As exogenous FA become more available, FA binding to CD36 dissociates Fyn, impairing its access to CD36-associated LKB1. The ensuing cytosolic enrichment in LKB1 promotes LKB1 activation of AMPK. The data support the concept of CD36 functioning as a component of signaling protein complexes with CD36 ligands differentially modulating protein associations within these complexes and consequently the access of CD36 partner kinases to downstream phosphorylation targets.

Evidence of CD36 regulation of AMPK in vivo was shown in fasted $CD36^{-/-}$ mice from the basally increased muscle and heart pAMPK, from the low RQ, and from the depletion of endogenous TG. Thus, while oxidation of exogenous FA, measured using FA analogs, was shown to be reduced in CD36-deficient mice and humans due to impaired FA uptake (3,5), oxidation of FA from endogenous supply would be enhanced. CD36 dysfunction, as occurs with chronic excess FA (21) or diabetes (22), might alter the lipid-sensing ability of AMPK, contributing to the etiology of lipid-associated metabolic complications.

In summary, this study documents the close coordination between CD36 and AMPK in the regulation of cellular FA metabolism. CD36 maintains basal AMPK quiescence, whereas FA-induced CD36 signaling activates AMPK, which disinhibits β-oxidation and recruits more CD36 to the sarcolemma. The positive reinforcement of FA catabolism during high FA supply would help to maintain cellular FA homeostasis. However, its dysfunction might contribute to the abnormalities of FA metabolism observed in diabetes and to the association of common CD36 variants with the metabolic syndrome (23).

Acknowledgments. The authors acknowledge the assistance of Alice Tong with mouse husbandry and genotyping and the Mouse Phenotyping Core and the Adipocyte Biology and Molecular Nutrition Core of the Nutrition and Obesity Research Center.

Funding. This study was supported by National Institutes of Health (NIH) grants R01-DK-033301, R01-DK-060022, and R01-DK-097608 and by National Natural Science Foundation of China grant 31371437. The Mouse Phenotyping Core and the Adipocyte Biology and Molecular Nutrition Core of the Nutrition and Obesity Research Center were supported by NIH grant P30-DK-056341.

Duality of Interest. No potential conflicts of interest relevant to this article were reported.

Author Contributions. D.S. designed the study, conducted the research, analyzed the data, and wrote the manuscript. J.S. and T.P. conducted the research and analyzed the data. R.W.G., R.H.E., X.S., and P.D.S. contributed to the data analysis or provided reagents. N.A.A. designed the study and wrote the manuscript. D.S. and N.A.A. are the guarantors of this work and, as such, had full access to all the data in the study and take responsibility for the integrity of the data and the accuracy of the data analysis.

References

1. Hardie DG. AMPK: a target for drugs and natural products with effects on both diabetes and cancer. Diabetes 2013;62:2164–2172

2. Shirwany NA, Zou MH. AMPK: a cellular metabolic and redox sensor. A minireview. Front Biosci (Landmark Ed) 2014;19:447–474

3. Glatz JF, Luiken JJ, Bonen A. Membrane fatty acid transporters as regulators of lipid metabolism: implications for metabolic disease. Physiol Rev 2010;90:367–417

4. Ruderman NB, Carling D, Prentki M, Cacicedo JM. AMPK, insulin resistance, and the metabolic syndrome. J Clin Invest 2013;123:2764–2772

5. Pepino MY, Kuda O, Samovski D, Abumrad NA. Structure-function of CD36 and importance of fatty acid signal transduction in fat metabolism. Annu Rev Nutr 2014;34:281–303

6. Ibrahimi A, Bonen A, Blinn WD, et al. Muscle-specific overexpression of FAT/CD36 enhances fatty acid oxidation by contracting muscle, reduces plasma triglycerides and fatty acids, and increases plasma glucose and insulin. J Biol Chem 1999;274:26761–26766

7. Dramane G, Abdoul-Azize S, Hichami A, et al. STIM1 regulates calcium signaling in taste bud cells and preference for fat in mice. J Clin Invest 2012;122:2267–2282

8. Sundaresan S, Shahid R, Riehl TE, Chandra R, Nassir F, Stenson WF, Liddle RA, Abumrad NA. CD36-dependent signaling mediates fatty acid-induced gut release of secretin and cholecystokinin. FASEB J 2013;27:1191–1202

9. Febbraio M, Abumrad NA, Hajjar DP, et al. A null mutation in murine CD36 reveals an important role in fatty acid and lipoprotein metabolism. J Biol Chem 1999;274:19055–19062

10. Hajri T, Hall AM, Jensen DR, et al. CD36-facilitated fatty acid uptake inhibits leptin production and signaling in adipose tissue. Diabetes 2007;56:1872–1880

11. Han X, Yang J, Cheng H, Ye H, Gross RW. Toward fingerprinting cellular lipidomes directly from biological samples by two-dimensional electrospray ionization mass spectrometry. Anal Biochem 2004;330:317–331

12. Kuda O, Pietka TA, Demianova Z, et al. Sulfo-N-succinimidyl oleate (SSO) inhibits fatty acid uptake and signaling for intracellular calcium via binding CD36 lysine 164: SSO also inhibits oxidized low density lipoprotein uptake by macrophages. J Biol Chem 2013;288:15547–15555

13. Smith BK, Jain SS, Rimbaud S, et al. FAT/CD36 is located on the outer mitochondrial membrane, upstream of long-chain acyl-CoA synthetase, and regulates palmitate oxidation. Biochem J 2011;437:125–134

14. Watt MJ, Steinberg GR, Chen ZP, Kemp BE, Febbraio MA. Fatty acids stimulate AMP-activated protein kinase and enhance fatty acid oxidation in L6 myotubes. J Physiol 2006;574:139–147

15. Han X, Cheng H, Mancuso DJ, Gross RW. Caloric restriction results in phospholipid depletion, membrane remodeling, and triacylglycerol accumulation in murine myocardium. Biochemistry 2004;43:15584–15594

16. Yamada E, Pessin JE, Kurland IJ, Schwartz GJ, Bastie CC. Fyn-dependent regulation of energy expenditure and body weight is mediated by tyrosine phosphorylation of LKB1. Cell Metab 2010;11:113–124

17. Mariotti A, Kedeshian PA, Dans M, Curatola AM, Gagnoux-Palacios L, Giancotti FG. EGF-R signaling through Fyn kinase disrupts the function of integrin alpha6beta4 at hemidesmosomes: role in epithelial cell migration and carcinoma invasion. J Cell Biol 2001;155:447–458

18. Miao WM, Vasile E, Lane WS, Lawler J. CD36 associates with CD9 and integrins on human blood platelets. Blood 2001;97:1689–1696

19. Garner AE, Smith DA, Hooper NM. Visualization of detergent solubilization of membranes: implications for the isolation of rafts. Biophys J 2008;94:1326–1340

20. Chen K, Febbraio M, Li W, Silverstein RL. A specific CD36-dependent signaling pathway is required for platelet activation by oxidized low-density lipoprotein. Circ Res 2008;102:1512–1519

21. Bastie CC, Hajri T, Drover VA, Grimaldi PA, Abumrad NA. CD36 in myocytes channels fatty acids to a lipase-accessible triglyceride pool that is related to cell lipid and insulin responsiveness. Diabetes 2004;53:2209–2216

22. Coort SL, Hasselbaink DM, Koonen DP, et al. Enhanced sarcolemmal FAT/CD36 content and triacylglycerol storage in cardiac myocytes from obese zucker rats. Diabetes 2004;53:1655–1663

23. Love-Gregory L, Abumrad NA. CD36 genetics and the metabolic complications of obesity. Curr Opin Clin Nutr Metab Care 2011;14:527–534